Special Publication ARAED-SP-92004

THERMAL DECOMPOSITION OF ENERGETIC MATERIALS. 4. DEUTERIUM ISOTOPE EFFECTS AND ISOTOPIC SCRAMBLING IN CONDENSED-PHASED DECOMPOSITION OF 1,3,5-TRINITROHEXAHYDRO-S-TRIAZINE

Richard Behrens, Jr.
Comubstion Research Facility
Sandia National Laboratories
Livermore, CA 94551

Suryanarayana Bulusu
ARDEC

February 1993

U.S. ARMY ARMAMENT RESEARCH, DEVELOPMENT AND ENGINEERING CENTER

Armament Engineering Directorate

Picatinny Arsenal, New Jersey

The views, opinions, and/or findings contained in this report are those of the authors(s) and should not be construed as an official Department of the Army position, policy, or decision, unless so designated by other documentation.

The citation in this report of the names of commercial firms or commercially available products or services does not constitute official endorsement by or approval of the U.S. Government.

Destroy this report when no longer needed by any method that will prevent disclosure of its contents or reconstruction of the document. Do not return to the originator.

REPORT DOCUMENTATION PAGE	Form Approved OMB No. 0704-0188

1. AGENCY USE ONLY (Leave blank)	2. REPORT DATE	3. REPORT TYPE AND DATES COVERED
	February 1993	Technical

4. TITLE AND SUBTITLE

Thermal Decomposition of Energetic Materials. 4. Deuterium Isotope Effects and Isotopic Scrambling in Condensed-Phase Decomposition of 1,3,5-Trinitrohexahydro-s-triazine

5. FUNDING NUMBERS

6. AUTHOR(S)

Richard Behrens, Jr., Sandia National Laboratories
Suryanarayana Bulusu, ARDEC

7. PERFORMING ORGANIZATION NAME(S) AND ADDRESSES(S)

Combustion Research Facility
Sandia National Laboratories
Livermore, CA 94551

ARDEC, AED
Energetics & Warheads Div (SMCAR-AEE)
Picatinny Arsenal, NJ 07806-5000

8. PERFORMING ORGANIZATION REPORT NUMBER

Special Publication
ARAED-SP-92004

9.SPONSORING/MONITORING AGENCY NAME(S) AND ADDRESS(S)

ARDEC, IMD
STINFO Br (SMCAR-IMI-I)
Picatinny Arsenal, NJ 07806-5000

10. SPONSORING/MONITORING AGENCY REPORT NUMBER

11. SUPPLEMENTARY NOTES

12a. DISTRIBUTION/AVAILABILITY STATEMENT

Approved for public release; distribution is unlimited.

12b. DISTRIBUTION CODE

13. ABSTRACT (Maximum 200 words)

The inter- versus intramolecular origin of the products formed in the thermal decomposition of 1,3,5-trinitrohexahydro-s-triazine (RDX) has been traced by isotopic crossover experiments using mixtures of differently labeled analogues of RDX. The isotopic analogues of RDX used in the experiments include ^{2}H, ^{13}C, ^{15}N, and ^{18}O. The fraction of isotopic scrambling and the extent of the deuterium kinetic isotope effect (DKIE) are reported for the different thermal decomposition products. Isotopic scrambling is not observed for the N-N bond in N_2O and only in small amounts (7%) in the C-H bonds in CH_2O, consistent with a mechanism of their formation through methylene nitramine precursors. A product, oxy-s-triazine (OST, $C_3H_3N_3O$), does not undergo isotopic scrambling in H/D, $^{14}N/^{15}N$, or $^{13}C/^{18}O$ experiments, and its rate of formation exhibits a DKIE of 1.5. These results are consistent with the formation of OST via unimolecular decomposition of RDX. Another product, *1-nitroso-3,5-dinitrohexahydro-s-triazine* (ONDNTA, $C_3H_6N_6O_5$), is found to be formed with complete scrambling of the N-NO bond, suggesting an N-N bond cleavage and a radical recombination process in its formation. One of the hydrogen containing products, H_2O, exhibits a DKIE of 1.5 ± 0.1. In contrast, CH_2O and ONDNTA have DKIEs of 1.05 ± 0.1 and 1.05 ± 0.2, respectively, indicating that hydrogen transfer is not involved in the rate-limiting step of the reaction pathway leading to the formation of these products.

14. SUBJECT TERMS

RDX, OST, ONDNTA, Isotope effect, Isotopic scrambling, Thermal decomposition

15. NUMBER OF PAGES
14

16. PRICE CODE

17. SECURITY CLASSIFICATION OF REPORT	18. SECURITY CLASSIFICATION OF THIS PAGE	19. SECURITY CLASSIFICATION OF ABSTRACT	20. LIMITATION OF ABSTRACT
UNCLASSIFIED	UNCLASSIFIED	UNCLASSIFIED	SAR

CONTENTS

TABLES

FIGURES

Introduction

The cyclic nitramines 1,3,5-trinitrohexahydro-*s*-triazine (RDX, I) and octahydro-1,3,5,7-tetranitro-1,3,5,7-tetrazocine (HMX, II)

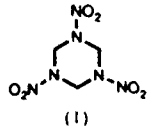

(I)

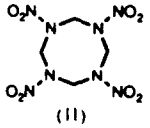

(II)

are energetic ingredients that are used in various propellants and explosives. Understanding the complex physicochemical processes that underlie the combustion of these materials can lead to methods for modifying the propellant and explosive formulations in order to obtain better ignition, combustion, or sensitivity properties. Our work strives to provide a link between the physical properties and molecular structures of different nitramines and their combustive behavior. This requires the understanding of the reaction kinetics and transport processes in both the gas and condensed phases. The thrust of our work is to obtain a better understanding of physical processes and reaction mechanisms that occur in the condensed phase so that the identity and rate of release of the pyrolysis products from the condensed phase can be predicted, as a function of pressure and heating rate, based on the physical properties and molecular conformation of the material.

Reviews[1] of the literature on RDX and HMX have discussed the roles of unimolecular decomposition and autocatalysis on the thermal decomposition of these compounds. Previous work,[2-5] has shown that HMX decomposes in the condensed phase and that the identity and rates of release of the pyrolysis products are determined by complex physical procesess coupled with several different chemical decomposition mechanisms.[4,5] The physical processes include the formation and containment of the gaseous

pyrolysis products in bubbles within the HMX particles and the subsequent release of the gases as escape paths form within the HMX particles. The long containment time of decomposition products within the HMX particles allows secondary reactions between the decomposition products and HMX.

In contrast to HMX, RDX has a lower melting point (202 °C for RDX compared to ~280 °C for HMX), so that decomposition occurs primarily in the liquid phase with a faster release of the gaseous products from the sample than for HMX. Although both RDX and HMX have been found[4,6-8] to form H_2O, HCN, CO, CH_2O, NO, N_2O, amides (e.g., methylformamide), a nonvolatile residue (NVR), and the mononitroso analogues of the parent compound (1-nitroso-3,5,7-trinitro-1,3,5,7-tetrazocine (ONTNTA) from HMX and 1-nitroso-3,5-dinitrohexahydro-*s*-triazine (ONDNTA) from RDX), only in experiments with RDX[6,7,8b] have NO_2 and oxy-*s*-triazine (OST, III) been observed. Although the precise structure of OST has not been determined, it is likely to be one of the following structures:

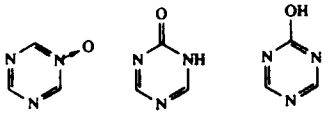

III

The two c-oxide structures are possibly prototropic tautomers. This paper presents the results of measurements of isotopic scrambling of products from mixtures of isotopic analogues of RDX and of the observed deuterium kinetic isotope effects (DKIE). Together, these two types of results are used to probe the decomposition mechanisms of RDX.

The basic mechanisms that have been considered in the past to describe the decomposition of RDX fall broadly into three categories. These include the least energy pathway[9] involving the N–N bond cleavage

$$RDX \rightarrow NO_2 + H_2CN + 2H_2C{=}N{-}NO_2 \qquad (R1)$$

the concerted triple scission pathway

$$RDX \rightarrow 3H_2C{=}N{-}NO_2 \qquad (R2)$$

found in IRMPD experiments with RDX,[10] and the HONO elimination pathway[11]

$$RDX \rightarrow 3HONO + 3HCN \qquad (R3)$$

Secondary reactions of methylenenitramine

$$H_2C{=}N{-}NO_2 \rightarrow HONO + HCN \qquad (R4)$$

$$H_2C{=}N{-}NO_2 \rightarrow CH_2O + N_2O \qquad \text{(C–N bond scission)} \qquad (R5)$$

have been postulated for many years to explain the formation of HCN, CH_2O, and N_2O and have been shown to occur in the infrared multiphoton dissociation (IRMPD) experiments[10] with RDX.

Recent thermal decomposition studies of RDX[7,8] have shown that it is also important to account for the formation of OST and ONDNTA in the decomposition mechanism since the final products formed during the decomposition of these materials may be formed via these intermediates. To address these issues, we use mixtures of isotopically labeled compounds to track the breaking and formation of chemical bonds that lead to the generation of pyrolysis products from the thermal decomposition of RDX. We also probe the role of carbon–hydrogen bonds in the formation of the different decomposition products by comparing changes in their rates of formation due to the DKIE. We present results from simultaneous thermogravimetric modulated beam mass spectrometry (STMBMS) measurements from RDX, RDX-d_6, and mixtures of unlabeled RDX (RDX-ul) with the isotopically labeled analogues, RDX-d_6, RDX-^{13}C, and RDX-$^{15}N_6$, and those between RDX-^{13}C and RDX-^{18}O. The same measurements are used to determine the DKIE on the pyrolysis products during the course of the decomposition and to determine the amount of isotopic scrambling that occurs in forming the pyrolysis products from different isotopic mixtures of RDX. We report the calculation fraction of isotopic scrambling observed for most of the products formed in experiments with different combinations of the labeled RDX compounds.

TABLE I: Experimental Parameters[a]

compound	enrichment (%)	experiment reactant quantity (mg) 1	2	3	4
RDX-ul		2.04	2.68	3.35	
RDX-d_6	97.3	1.98	2.6		
RDX-$^{15}N_6$	98.5			3.53	
RDX-^{13}C	98.1				2.26
RDX-^{18}O	3.7				2.26
electron energy (eV)		18	20	20	20
orifice diam (cm)		0.002 54	0.002 54	0.002 54	0.002 54
temp range[b]		198–207	198–207	198–208	198–207

[a] All mixtures of isotopic analogues of RDX are recrystallized from an acetone solution. [b] Temperature range over which the decomposition of RDX occurs in °C. Heating rate for all experiments is 0.5 °C/min in the temperature range of the decomposition.

Experimental Section

Instrument Description. The STMBMS apparatus and basic data analysis procedure have been summarized in the previous paper[7] and are described more extensively elsewhere.[12,13]

Sample Preparation. Samples of RDX with different isotopic labels were synthesized by the general method previously reported elsewhere.[14] To obtain a given isotopic analogue, starting materials with the appropriate isotopic enrichment were employed. Briefly, the synthesis involves treating hexamine in a solution of acetic anhydride and glacial acetic acid maintained at 44 °C, with a "nitrolysis" mixture consisting of ammonium nitrate and 98–100% nitric acid. This reaction yields a mixture of HMX and RDX and the workup requires separation of the two products by extraction with ethylene dichloride in which RDX is much more soluble than HMX. Each product is then purified by multiple recrystallizations from aqueous acetone and characterized by melting points and ^{1}H-NMR and mass spectra.

The ^{15}N labeling of RDX is achieved by first synthesizing hexamine from $(CH_2O)_n$ and $^{15}NH_3$ (liberated from ammonium acetate and 30% aqueous KOH) and using $^{15}NH_4{}^{15}NO_3$ and $H^{15}NO_3$ in the nitrolysis mixture. $H^{15}NO_3$ is prepared by vacuum distillation at low temperature from $Na^{15}NO_3$ and CP H_2SO_4. ^{13}C enrichment uses $(^{13}CH_2O)_n$ as starting material for hexamine while ^{18}O labeling requires $NH_4N^{18}O_3$ and $HN^{18}O_3$ obtained as above.

Preparation of RDX-d_6. Deuterium labeling is achieved more economically by a recently reported[15] exchange method. This involves prior synthesis of 1,3,5-trinitroso-hexahydro-*s*-triazine (IV) by treating[16] hexamine in aqueous HCl with $NaNO_2$ at 0 °C and recrystallizing the precipitated product from ethyl alcohol (95%). This product is then subjected to base-catalyzed H–D exchange by refluxing in anhydrous CH_3OD (5 mL/(mmol of IV)) containing 1 μmol of potassium methoxide. After solvent removal the product is taken up in methylene chloride and washed free of base with D_2O. Evaporation of the solvent again gives 97% deuterium-labeled IV. Repetition of the exchange reaction a second time ensures a 99% D-labeled product.

Oxidation to RDX-d_6. A 1-g amount of IV is added slowly with stirring to 15 mL of CP H_2SO_4 maintained at −20 °C. With the temperature held at −20 °C, 4.6 mL of 100% HNO_3 is added to it slowly over an hour. After being stirred for another 30 min, the solution is gradually warmed to 18 °C and poured over crushed ice (100 g). The RDX-d_6 that is obtained in 90% yield is washed free of acid with water and recrystallized from aqueous acetone.

The isotopic enrichment of each of the isotopomers used in the experiments is listed in Table I.

Samples for experiments with mixtures of isotopic analogues of RDX are prepared by mixing the ingredients in acetone solution. The samples mixed in acetone solution are prepared by dissolving approximately equal quantities of the two isotopomers in solution

and then letting the solvent evaporate. The amounts of each ingredient used in each experiment are listed in Table I.

For each mixed-isotope experiment listed in Table I, experiments were run on each of the isotopic analogues separately. The results from these experiments are used to check for the presence of ion signals at m/z values that should originate only from the mixing of isotopes in the scrambling experiments. If there is a measurable amount of ion signal present in the experiments with the separate isotopic analogues, then the results of the separate experiments are used to correct the data from the isotope scrambling experiments.

Analysis

The data analysis procedures used for identifying the pyrolysis products and determining their rates of formation have been described previously.[12,13,17] Since this paper examines the extent of isotopic scrambling and the DKIE on the relative rates of formation of the various products, it is sufficient to compare the ratios of the ion signals measured at different m/z values for the various products. The structures of the more complex decomposition products discussed in this paper are reasonable assumed structures based on the mass spectra of different isotopic analogues of RDX.[7] OST has been investigated previously by tandem mass spectrometry,[8] but a definitive structure could not be assigned.

The relative size of the ion signals at the different m/z values associated with an individual decomposition product is dependent on the amount of each isotopically labeled analogue used in the experiment, the fraction of each analogue that participates in forming isotopically scrambled products, the cracking factors in the ion fragmentation process, and the fraction of isotopic enrichment in each isotopically labeled analogue.

The amount of each product isotopomer formed from the decomposition of a mixture of r mol of isotopomer 1 and s mol of isotopomer 2 of RDX is given by

$$r\mathrm{RDX}_1 + s\mathrm{RDX}_2 \rightarrow x\kappa r(1-f)\mathrm{A}_{11} + \kappa s(1-f)\mathrm{A}_{22} + \kappa f(xr+s)\mathrm{A}_{12} \quad \text{(R6)}$$

where A represents the type of pyrolysis product, A_{11} and A_{22} are formed from RDX_1 and RDX_2, respectively, A_{12} represents the set of mixed-isotope products, κ is the number of moles of product A formed per mole of RDX_2, x is the ratio of the number of moles of product A formed from RDX_1 to the number of moles of product A formed from RDX_2 (for deuterium-labeled RDX this corresponds to the DKIE factor), and f is the fraction of the product molecules produced from either RDX_1 or RDX_2 that participate in isotope scrambling. For experiments in which the isotopomers are not completely labeled, Reaction R6 is modified to account for the fraction of enrichment of each of the isotopomers used in the scrambling experiment. The predicted combinations of the isotopes of the different elements in each of the mixed-product isotopomers are assumed to be random over the available molecular configurations.

After the expression for the amount of different product isotopomers is determined, it is combined with the following expression that accounts for the relative number of ions formed in the mass spectrometer at different m/z values from the product isotopomer

$$S_k^+ = \sum_{i=1}^{\#\ \text{isotopomers}} F_{i,k} A_i^+ \quad (1)$$

where S_k^+ is the ion signal at $m/z = k$, A_i^+ is the total number of ions formed from the isotopomer A_i with mass m_i, and $F_{i,k}$ is the fraction of the total number of ions formed from A_i that appear at $m/z = k$. The $F_{i,k}$ terms are assumed to be independent of the isotopic mass in the product molecules except for the case in which the ion fragmentation involves the scission of a bond with a hydrogen isotope. For the hydrogen bond breaking cases separate fragmentation terms $F_{i,k}$ are used for each product isotopomer.

On the basis of reaction R6, eq 1, and the isotopic enrichment fractions for the RDX analogues used in the experiments, expressions for the amount of ion signal at each different m/z value associated with a decomposition product are formulated. These expressions are then used to construct equations based on the ratios of the ion signals at different m/z values for a given product. These equations are then solved for the values of f and x.

Prior to using the data from the isotopic scrambling experiments to determine the values of f and x, the ion signals at m/z values in which isotopic scrambling is expected are corrected for ion signals that may be present from a source other than the product of interest. The correction is accomplished by determining the ratio of the unexpected signal at the desired m/z value to an appropriate reference signal from either an RDX or RDX product ion fragment (or the corresponding isotopic analogue) from experiments with individual isotopic analogues and by applying the correction factor to the results from the isotopic scrambling experiment.

TABLE II: H_2O Isotopic Scrambling Results

isotopes	expt no.	m/z	rel intens	temporal correln[b]
H/D	2[a]	18	64 ± 11	Y
		19	100	Y
		20	24 ± 3	Y

[a] Results for isotopic scrambling of H_2O from experiment 1 are not included because of interference from an extraneous signal at m/z = 18. [b] Y indicate that the ion signals at these m/z values are temporally correlated with all the other m/z values listed in the experiment.

TABLE III: CH_2O Isotopic Scrambling Results

isotopes	expt no.	m/z	rel intens	temporal correln[c]
H/D	1	29	49 ± 3	Y
		31	15 ± 3[a]	Y
		32	100 ± 3	Y
	2	29	61 ± 5	Y
		31	16 ± 5	Y
		32	100 ± 5	Y
$^{13}C/^{18}O$	4	31	100	Y
		32	5.4 ± 0.6	Y
		33	1.4 ± 0.1[b]	Y

[a] Corrected for 31^+ contribution from pure RDX-ul. [b] Corrected for the 33^+ contribution observed in a separate experiment with RDX-^{13}C. The correlations are made using the CH_2O (^{13}C m/z = 31) signal for normalization. [c] Y indicates that the ion signals at these m/z values are temporally correlated with all the other m/z values listed in the experiment.

TABLE IV: N_2O Isotopic Scrambling Results

isotopes	expt no.	m/z	rel intens[a]	temporal correln[b]
$^{14}N/^{15}N$	3	44	100 ± 10	Y
		45	−4.1 ± 2	na
		46	93.9 ± 11	Y

[a] The ion signal at each m/z value is corrected for overlapping ion signals that are observed in experiments with individual RDX-ul and RDX-$^{15}N_6$ samples. [b] Y indicates that the ion signals at these m/z values are temporally correlated with all the other m/z values listed in the experiment.

Results

Table I summarizes the amounts of isotopic analogues of RDX used in the mixed-isotopomer experiments and the isotopic enrichment of the isotopic analogues. The isotopic scrambling results for the products H_2O, CH_2O, N_2O, OST, and ONDNTA are summarized in Tables II–VI, while the mixing fractions (crossover), f, and the observed DKIEs, x, for the deuterium labeled products are presented in Table VII. Figures 1–6 show the relative intensities as a function of temperature and the temporal correlations of groups of ion signals at various m/z values that are used to determine the extent of the DKIE and isotopic scrambling for the decomposition products formed from RDX. Since the heating rates were linear with time, the curves also reflect the temporal correlations between the ions signals. All of the data presented

TABLE V: Oxy-*s*-triazine (OST, $C_3H_3N_3O$) Isotopic Scrambling Results

isotopes	expt no.	m/z	rel intens	temporal correln[b]
H/D	1	97	100 ± 3	N
		98	4 ± 3	na
		99	4 ± 3	na
		100	(45–71) ± 3	N
	2	97	100 ± 2	Y
		98	3.1 ± 2.1	na
		99	2.8 ± 0.4	na
		100	(38–59) ± 2	Y
$^{14}N/^{15}N$	3	97	100 ± 2	Y
		98	1 ± 2	na
		99	1 ± 2	na
		100	100 ± 2	Y
$^{13}C/^{18}O$	4	97	85.4 ± 4	Y
		99	5.4 ± 0.5	Y
		100	100.0	Y
		102	0.8 ± 0.8	N

[a] Ion signals at m/z values of 98 and 102 have been corrected for the ion signal due to fragmentation of RDX in the ionizer of the mass spectrometer. [b] Y indicates that the ion signals at these m/z values are temporally correlated with all the other m/z values listed in the experiment. N indicates that the ion signals are not temporally correlated with other ion signals in the group.

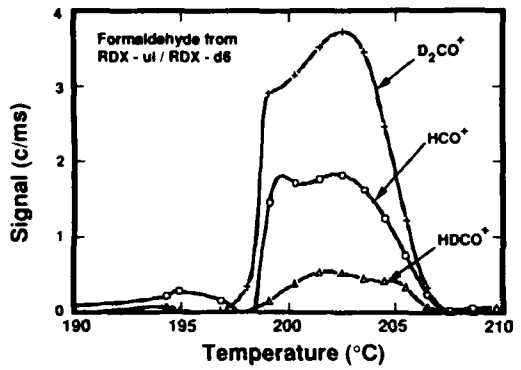

Figure 1. Ion signals, formed in the mass spectrometer, from CH_2O and its isotopic analogues formed during the decomposition of a mixture of RDX-ul and RDX-d_6 (experiment 1 in Table I). Between 193 and 210 °C the heating rate of the sample is 0.5 °C/min. The rapid increase in the rate of evolution of CH_2O at 198 °C occurs as the sample melts.

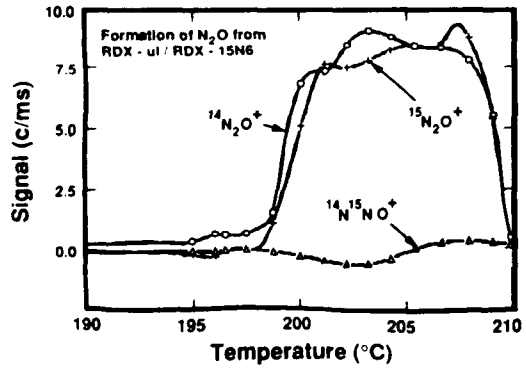

Figure 2. Ion signals, formed in the mass spectrometer, from N_2O and its isotopic analogues formed during the decomposition of a mixture of RDX-ul and RDX-$^{15}N_6$ (experiment 3 in Table I). Between 195 and 210 °C the heating rate of the sample is 0.5 °C/min. The rapid increase in the rate of evolution of N_2O at 199 °C occurs as the sample melts.

in Figures 1–6 clearly show that the decomposition products are first observed in significant quantities when RDX starts to melt at 198 °C. As shown in the previous paper,[7] decomposition of RDX is significantly inhibited in the solid phase.

H_2O. Scrambling of the hydrogen isotopes is observed in the formation of water from a mixture of RDX-ul and RDX-d_6.

TABLE VI: ONDNTA ($C_3H_6N_3(NO_2)_2NO$) Isotopic Scrambling Results

isotopes	expt no.	m/z[a]	rel intens[b]	temporal correln[c]
H/D	1	132	100 ± 14	Y
		133	7 ± 5	Y
		134	0[d]	na
		135	5 ± 2	Y
		136	90 ± 5	Y
	2	132	97 ± 19	Y
		133	7 ± 4	Y
		134	0[d]	na
		135	8 ± 1	Y
		136	86 ± 3	Y
$^{14}N/^{15}N$	3	132	(90–98) ± 17	N
		133	(95–70) ± 5	Y-135
		134	0[d]	na
		135	(86–69) ± 5	Y-133
		136	(85–94) ± 6	n

[a] The m/z values are for an ion formula of $C_2H_4N_2(NO)(NO_2)$ that is formed by the fragmentation of ONDNTA in the ionizer of the mass spectrometer. [b] The ion signals at all of the m/z values have been corrected for contributions from fragmentation of RDX in the ionizer of the mass spectrometer. In addition, the ion signals at m/z values of 133 and 135 have been corrected for contributions from isotopomers that arise directly from the individual isotopic analogues of ONDNTA in the absence of scrambling. [c] Y indicates that the ion signals at these m/z values are temporally correlated with all the other m/z values listed in the experiment. N indicates that the ion signals are not temporally correlated with other ion signals in the group. Y–no. indicates that the ion signal is correlated with another m/z value in the group indicated by the number. [d] There is no evidence of transfer of two atoms between the product molecules.

TABLE VII: Mixing Fractions (f) and DKIE (x) Results from RDX Isotopic Scrambling Experiments

decomposn products	scrambled isotopes	f	x[a]
H_2O	H/D	1.1 ± 0.1	1.5 ± 0.1
CH_2O	H/D	0.075 ± 0.02	1.05 ± 0.1
	$^{13}C/^{18}O$	0.45 ± 0.07	
N_2O	$^{15}N_6/^{14}N_6$	−0.04 ± 0.03	
OST	H/D	0 ± 0.05	2.2–1.3[b]
	$^{15}N/^{14}N$	0 ± 0.05	
	$^{13}C/^{18}O$	0 ± 0.05	
ONDNTA	H/D	0.25 ± 0.05	1.05 ± 0.2
	$^{15}N_6/^{14}N_6$	1.0–0.61[c]	

[a] The values for x are calculated only for the H/D exchange experiments. [b] The DKIE for OST decreases as the sample undergoes decomposition due to the increase in the amount of RDX-d_6 relative to the amount of RDX-ul. [c] The fraction of NO that exchanges during the formation of ONDNTA decreases as the sample size decreases.

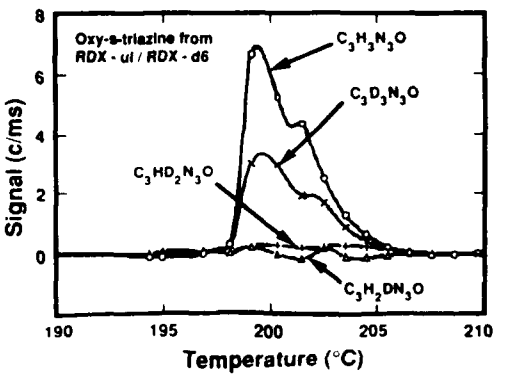

Figure 3. Ion signals, formed in the mass spectrometer, from oxy-*s*-triazine and its isotopic analogues formed during the decomposition of a mixture of RDX-ul and RDX-d_6 (experiment 1 in Table I). Between 193 and 210 °C the heating rate of the sample is 0.5 °C/min. The rapid increase in the rate of evolution of OST at 198 °C occurs as the sample melts.

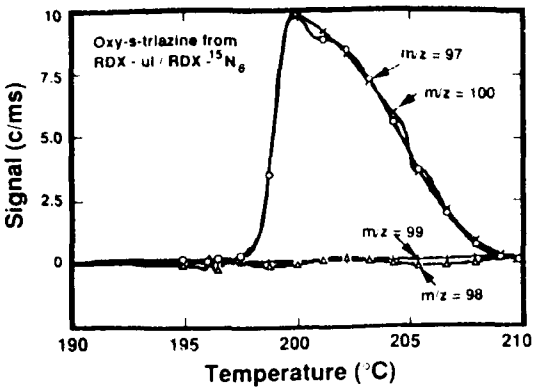

Figure 4. Ion signals, formed in the mass spectrometer, from oxy-*s*-triazine and its isotopic analogues formed during the decomposition of a mixture of RDX-ul and RDX-$^{15}N_6$ (experiment 3 in Table I). Between 195 and 210 °C the heating rate of the sample is 0.5 °C/min. The rapid increase in the rate of evolution of OST at 199 °C occurs as the sample melts.

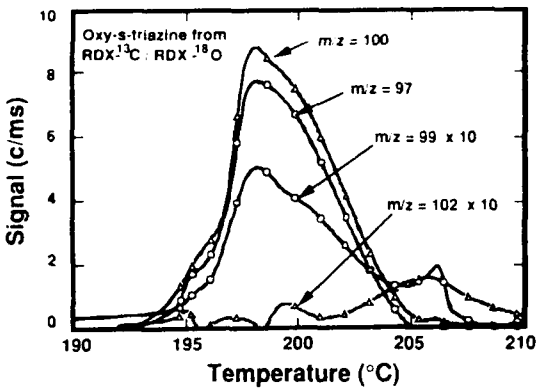

Figure 5. Ion signals, formed in the mass spectrometer, from oxy-*s*-triazine and its isotopic analogues formed during the decomposition of a mixture of RDX-^{13}C and RDX-^{18}O (experiment 4 in Table I). Between 195 and 210 °C the heating rate of the sample is 0.5 °C/min. The rapid increase in the rate of evolution of OST at 196 °C occurs as the sample melts.

Analysis of the data in Table II shows that the fraction of water that participates in mixing is 1.1 ± 0.1, which represents complete mixing and that the DKIE is 1.5 ± 0.1. Since low electron energies of 18 and 20 eV are used in the mass spectrometer, contributions from OD^+ are ignored. The results are calculated assuming only the molecular ions, H_2O^+, HDO^+, and D_2O^+ contribute to the measured signal. Since H and D exchange is rapid in water and is likely to occur before detection of the product, the observation of complete H/D scrambling does not necessarily imply that water is produced in a bimolecular reaction between either RDX itself or RDX and a decomposition product.

CH_2O. As indicated in Table VII the fraction of RDX that forms formaldehyde with hydrogen and deuterium exchange is about 7% for the experiments. It can be seen from Figure 1 that there is a high degree of temporal correlation between the ion signals from the isotopic analogues of formaldehyde. The observed DKIE for formaldehyde formation is 1.05 ± 0.1, which implies no deuterium kinetic isotope effect. The ion signals used in the analysis are for m/z values of CH_2O^+, CHO^+, and their isotopic analogues. Measured ion fragmentation factors for CH_2O and CD_2O were used to calculate the ratio of CHO^+/CH_2O^+ and CDO^+/CD_2O^+ formed in the ionization process.

Experiment 4 with a mixture of RDX-^{13}C and RDX-^{18}O shows that 45 ± 7% (Table VII) of the formaldehyde formed is from mixing between the two differently labeled RDX analogues. However, scrambling of ^{13}C and ^{18}O in formaldehyde may be the result of polymerization and depolymerization of formaldehyde after its initial formation and prior to its detection. The ion signals of $^{13}CH_2O$ (31), $CH_2{}^{18}O$ (32), and $^{13}CH_2{}^{18}O$ (33) were used to calculate the value for f.

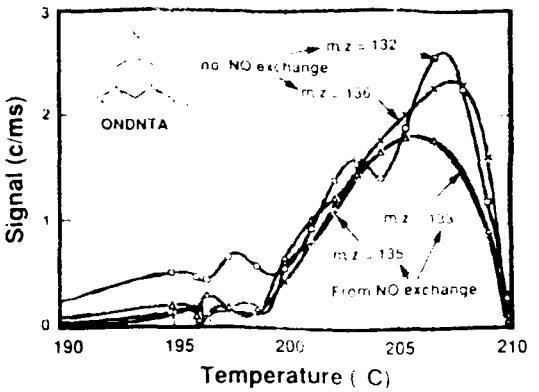

Figure 6. Ion signals, formed in the mass spectrometer, from ONDNTA and its isotopic analogues formed during the decomposition of a mixture of RDX-ul and RDX-$^{15}N_6$ (experiment 3 in Table I). Between 195 and 210 °C the heating rate of the sample is 0.5 °C/min. The larger variation in the ion signal at m/z = 132 is due to the large correction that was made to the signal for the contribution of the $CH_2N_2(NO)^+$ ion dissociation fragment formed from evaporating RDX.

N_2O. Experiment 3 (Table IV) with a mixture of RDX-ul and RDX-$^{15}N_6$ shows that none of the N_2O is formed from mixing between the two differently labeled RDX analogues. The ion signals of $^{14}N_2O^+$, $^{14}N^{15}NO^+$, and $^{15}N_2O^+$ (Figure 2) are used to calculate the mixing fraction.

OST. Three different kinds of isotopic scrambling experiments were used to derive mixing information for OST. The results are tabulated in Table V and shown in Figures 3-5. Analysis of the data presented in Table V shows *no mixing in any of these experiments*.

The experiments with RDX-ul and RDX-d_6 (Figure 3, Table VII) show a strong DKIE. The relative size of the DKIE ranges from 2.2 during the initial stage of formation of OST down to 1.3 at the final stage of formation of OST. This decrease in the DKIE is probably due to the increase in the relative amount of RDX-d_6 compared to RDX-ul as the sample decomposes.

ONDNTA. ONDNTA represents a product (MW 206) that is formed by the net loss of a single atom (oxygen) from RDX. The results from two different kinds of isotopic scrambling experiments for ONDNTA are tabulated in Table VI, and the results of the $^{14}N/^{15}N$ isotopic exchange measurements from ONDNTA are shown in Figure 6. The isotopic analysis of this product from the mixing experiments was based on its major fragment ion, m/z = 132 ($C_2H_4N_4O_3$) and it isotopic variants.

The data indicate that 25 ± 5% of the RDX participates in scrambling of H and D in the formation of ONDNTA, in spite of the fact that the product results from the loss of a single oxygen atom. But since there is no DKIE observed in the formation of this product, hydrogen is not involved in the rate-determining step for this product.

The $^{14}N/^{15}N$ mixing in the ONDNTA product can be readily seen in Figure 6. During the initial stages of the decomposition, the ion signals at m/z values of 132, 133, 135, and 136 are approximately equal, this indicating that the mixing is complete with respect to the N–NO bond, whereas, during the latter stages of the decomposition, the relative sizes of the ion signals at m/z values of 132 and 136 are larger compared to the ion signals at m/z values of 133 and 135, thus indicating that the extent of RDX that participates in mixing with respect to the N–NO bond falls to 60%.

Other Products. Scrambling of the C–N bonds in HCN and the amides has not been examined in this study. No isotopic scrambling is observed in the undecomposed RDX that evaporates from the reaction cell.

Discussion

As indicated in the Introduction, this paper focuses attention on the deuterium kinetic isotope effects and isotopic scrambling results of the decomposition products from mixtures of isotopically labeled RDX samples (Table I). However, it is helpful and

cessary to interpret these results in a broader perspective taking o account the relative amounts of all the products (see previous per), the role of physical factors, and a comparison to similar ta obtained from HMX. While the use of isotopes has been lpful in identifying several product species in these decomposition idies and the bond-making and bond-breaking processes, they o uncover inherent limitations in their use to draw detailed nclusions about reaction mechanisms.

It has already been stressed in the preceding papers in this series it several decomposition channels can be identified in both MX and RDX decomposition. In view of this, it is pertinent consider the relative importance of these channels of decomsition and understand the similarities and differences between MX and RDX imposed by the respective structural similarities l differences in physical properties (see Introduction).

N_2O and CH_2O. In RDX decomposition, only a small amount isotopic scrambling was observed for the C–H bonds of formlehyde (Table VII and Figure 1) and none was observed for N–N bonds in N_2O (Table VII and Figure 2), which are two ijor products. This is consistent with previous work[18] on DX-($^{15}NO_2$)$_3$ in which it was found that N_2O consisted mainly the ^{14}N–^{15}N–O configuration. If the N–N bond is broken in reaction path that leads to the formation of N_2O from RDX, n the results with RDX-$^{15}N_6$/RDX-ul should have shown mixed topes. That this was not the case (Table IV) shows clearly that, in the case of HMX, N_2O formed in the decomposition oriiates both directly from the parent molecule and indirectly ou:i an intermediate (ONDNTA) without rupture of the N–N nd.

While the C–H bonds in CH_2O exhibit only a minor degree mixing, the $^{13}C/^{18}O$ atoms showed 45% scrambling. This means it 45% of all the C–O bonds in the CH_2O product molecules formed from atoms drawn from different isotopic molecules. owever, this scrambling can readily occur in a CH_2O polymzation–depolymerization process any time prior to exiting from reaction cell. In the case of HMX the degree of mixing is n higher[5] (80%) presumably because CH_2O is held for longer iods within the solid particles compared to the decomposition RDX in a melt. The minor amount (<7%) of H–D scrambling, ewise, could have occurred after the initial formation of CH_2O e to the labile nature of the hydrogens. The lack of a DKIE CH_2O shows that C–H bond cleavage is not involved in the e-limiting step of the reaction pathway leading to its formation, is providing further evidence of several parallel reaction thways controlling the decomposition of RDX.

The isotopic scrambling results of N_2O and CH_2O, taken toher, point in the direction of a methylenenitramine decomsition to N_2O and CH_2O (reactions R1, R2, and R5) as in the e of IRMPD of RDX.[10] However, in the IRMPD gas-phase idy

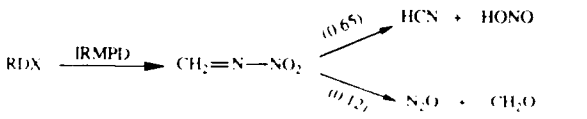

N_2O and CH_2O channel was not as dominant. In light of the ee primary decomposition pathways of RDX in the liquid phase it lead to the formation of N_2O this difference is not surprising. ost of the N_2O formed in the decomposition of RDX in the uid phase occurs either through the ONDNTA intermediate 42%) or through the catalyzed decomposition of RDX (~ %). Only a small fraction (~15%) of the N_2O appears to be med directly from RDX. Whether the N_2O formed via either ONDNTA pathway or the catalytic pathway passes through nethylenenitramine intermediate is uncertain at this point due a lack of any evidence of its formation during the decomposition RDX in the liquid phase.

H_2O Formation. The H_2O formation rate displays a strong ietic isotope effect (Table VII), suggesting it is formed in a action pathway, such as (R7), in which hydrogen is involved the rate-limiting step.

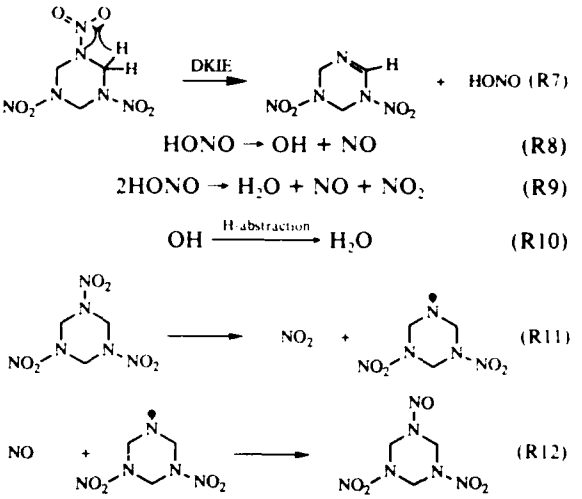

In this scheme, reaction R7 generates HONO accompanied by a primary kinetic isotope effect with deuterium label since a C–H bond scission is necessary. HONO, under reaction conditions, can undergo one or both of the two possible reactions, R8 and R9. In the former case, a hydroxyl radical is generated which on hydrogen abstraction (R10) yields H_2O as a product. Alternatively, the decomposition R9 can directly yield H_2O and two oxides of nitrogen, all of which have been detected among the products. The latter may be expected to seek other radical species to react with, such as the radical left behind on loss of an NO_2 group from RDX (R11). In this case, NO_2 will reform the RDX molecule while NO will lead to the formation of ONDNTA (R12) detected in the products.

ONDNTA. It is interesting that the ONDNTA formation as a product (Tables VI and VII) shows a substantial mixing of the nitrogen isotopes making up the N–NO bond and 25% mixing of H/D isotopes. The former is expected from R12 but it is not immediately apparent why H/D mixing is observed. The explanation for this may be that the hydrogens next to a nitroso group become labile (acidic) and exchangeable. In fact, this exchangeable nature of the hydrogens is taken advantage of in the synthesis of RDX-d_6 (see Experimental Section).

There is also NMR evidence[19] showing a substantial contribution of the resonance structure with charge localization on the ring nitrogen atom that would make the adjacent hydrogen more acidic and susceptible to hydrogen abstraction promoting decomposition of ONDNTA in the earlier stages of the reaction (see previous paper) due to reaction with other decomposition products.

The mixing of the nitrogen isotopes in the N–NO bond of course suggests the breaking of the N–NO_2 bond and the re-forming of it with a nitroso group. This mechanism is quite analogous to the one proposed for the formation of dimethylnitrosamine.[20] A radical addition, R$^{\bullet}$, to one of the oxygens of the nitro group followed by loss of the RO group to give nitroso–amine as proposed by Melius[21] is not valid here since it would not predict mixing of isotopes in the N–N bond.

OST. Oxy-*s*-triazine has proved to be a most intriguing product from RDX to rationalize.

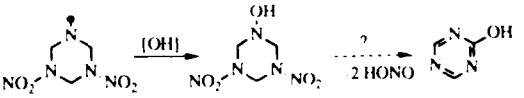

It would be reasonable to expect the radical produced in reaction 11 to pick up a hydroxyl group and eventually lead to OST by loss of two HONO molecules and internal bond rearrangement. However, the first objection to this would be the excess hydrogen atom on the ring. But, more importantly, OST is unique in that it fails to show mixing of any of the isotopes used (H/D, $^{14}N/^{15}N$, or $^{12}C/^{16}O$). This requires that it be formed in a strictly intramolecular process. It appears, therefore, that OST represents an additional decomposition pathway that is most likely a unimo-

lecular one. It can be seen in Figures 3–5 that the signal from OST abruptly increases at the melting point of RDX and then progressively decays as the sample is consumed. In order to take place, this reaction has to result in a loss of two HONO molecules and an HNO radical by the RDX molecule.

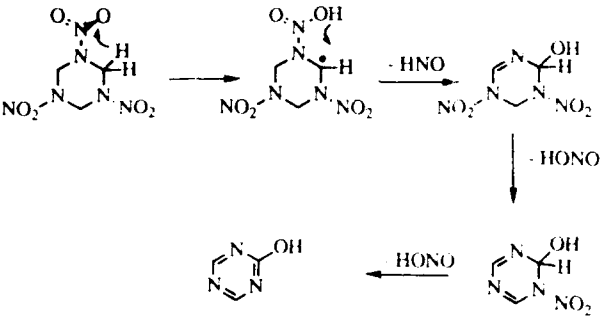

This reaction route to OST accounts for the total lack of mixing of the isotopes, the consequent intramolecular nature of the product, the unimolecular kinetics apparent from Figures 3–5, and the observed DKIE. It is interesting to note that OST is the only decomposition product from RDX that solely exhibits unimolecular decomposition kinetics (other products are produced by both the unimolecular and other decomposition pathways).

Summary

The results from isotope crossover experiments with RDX and the observed deuterium kinetic isotope effects (DKIE) lend further support for the four primary decomposition pathways described in the previous paper[7] and may be summarized as follows:

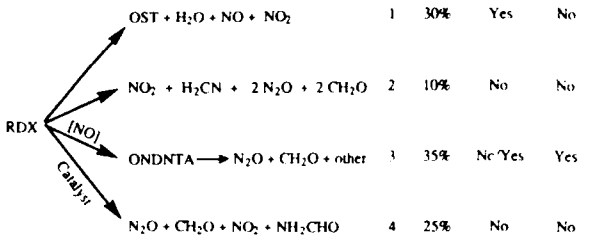

Two pathways are first-order reactions solely in RDX. Pathway 1 produces predominantly OST, NO, and H_2O and accounts for approximately 30% of the decomposed RDX and pathway 2 produces predominantly N_2O and CH_2O with smaller amounts of NO_2, CO, and NH_2CHO and accounts for 10% of the decomposed RDX. Pathway 3 consists of formation of ONDNTA by reaction between NO and RDX, followed by the decomposition of ONDNTA to predominantly CH_2O and N_2O. Pathway 4 consists of decomposition of RDX through reaction with a catalyst that is formed from the decomposition products of previously decomposed RDX. Reaction pathways 3 and 4 each account for approximately 30% of the decomposed RDX.

The lack of isotopic scrambling and the presence of a primary DKIE in OST support a unimolecular mechanism in pathway 1. The primary DKIE in the formation of OST shows the importance of intramolecular hydrogen transfer in the rate-limiting step that controls pathway 1.

Reaction pathway 3 is supported by the scrambling of $^{14}N/^{15}N$ in the nitroso group of the ONDNTA formed during the decomposition of RDX. In addition, the lack of a DKIE in the formation of ONDNTA also supports this pathway. Furthermore, the presence of H/D scrambling is consistent with the presence of more labile hydrogen on the neighboring carbon atom of the N–NO group in ONDNTA.

The lack of nitrogen scrambling in N_2O is consistent with the conclusion that methylene nitramine collapses to N_2O and formaldehyde without cleavage of the N–N bond. However, the lack of direct evidence of methylenenitramine makes its formation through this intermediate uncertain.

The lack of a DKIE in the formation of CH_2O supports the conclusion that hydrogen is not involved in the rate-limiting steps of pathways 2–4 that lead to its formation.

Unlike the case of HMX decomposition which is catalyzed by H_2O, there seems to be no evience of autocatalysis by H_2O in the RDX case. H_2O formation is not the sole contributor to the observed DKIE as in the case of HMX. It is, therefore, apparent that the decomposition details of RDX and HMX are significantly different due to the fact that the former occurs in the liquid phase and the latter in the solid phase. Furthermore, RDX undergoes isotopic scrambling of nitrogen in the formation of ONDNTA, whereas for the analogous compound in HMX, ONTNTA, only 25% of the molecules are formed by mixing of the nitrogen isotopes. This implies that the formation of ONTNTA in HMX is influenced by the "cage effect" in its solid-state decomposition, whereas the formation of ONDNTA in RDX occurs in the liquid phase and the cage effect does not play a role. This also predicts that if HMX is decomposed above its melting point, it also would exhibit more scrambling of the nitrogen isotopes.

Acknowledgment. The authors thank M. G. Mitchell and K. A. Morrison for assistance in running the experiments and collecting the data and J. R. Autera for assistance in the isotopic syntheses. This research was supported by the U.S. Army Research Office and the U.S. Army ARDEC.

References and Notes

(1) For reviews, see: (a) Boggs, T. L. The Thermal Decomposition Behavior of Cyclotrimethylene-trinitramine (RDX) and Cyclotetramethylene-tetranitramine (HMX). In *Fundamentals of Solid-Propellant Combustion*; Kuo, K. K., Summerfield, M., Eds.; Progress in Astronautics and Aeronautics, Vol. 90; AIAA Inc.: New York, 1984; p 121. (b) Fifer, R. A. Chemistry of Nitrate Ester and Nitramine Propellants. In *Fundamentals of Solid-Propellant Combustion*; Kuo, K. K., Summerfield, M., Eds.; Progress in Astronautics and Aeronautics, Vol. 90; AIAA Inc.: New York, 1984; p 177. (c) Schroeder, Michael A. Critical Analysis of Nitramine Decomposition Data: Product Distributions from HMX and RDX. U.S. Army Ballistic Research Laboratory Report BRL-TR-2659, 1985. (d) Schroeder, Michael A. Critical Analysis of Nitramine Decomposition Data: Activation Energies and Frequency Factors for HMX and RDX Decomposition. U.S. Army Ballistic Research Laboratory Report BRL-TR-2673, 1985.

(2) Bulusu, S.; Graybush, R. J. Proceedings of the 36th International Congress on Industrial Chemistry, Brussels, Belgium, 1967. *C. R. Ind. Chim. Belge* **1967**, *32*, 647.

(3) Karpowicz, R. J.; Brill, T. B. *AIAA J.* **1982**, *20*, 1586.

(4) Behrens, R., Jr. *J. Phys. Chem.* **1990**, *94*, 6706.

(5) Behrens, R., Jr.; Bulusu, S. *J. Phys. Chem.* **1991**, *95*, 5838.

(6) Behrens, R., Jr. *Proceedings of the 23rd JANNAF Combustion Meeting*; Langley, VA; CPIA Publication No. 457; Chemical Propulsion Information Agency: Laurel, MD, 1986; pp 231–240.

(7) Behrens, R., Jr.; Bulusu, S. *J. Phys. Chem.*; previous paper in this issue.

(8) (a) Snyder, A. P.; Liebman, S. A.; Bulusu, S.; Schroeder, M. A.; Fifer, R. A. *Org. Mass Spectrom.* **1991**, *26*, 1109. (b) Snyder, A. P.; Kremer, J. H.; Liebman, S. A.; Schroeder, M. A.; Fifer, R. A. *Org. Mass Spectrom.* **1989**, *24*, 15.

(9) Melius, C. F. *J. Phys., Colloque C4* **1987**, *48*, 341.

(10) Zhao, X.; Hintsa, E. J.; Lee, Y. T. *J. Chem. Phys.* **1988**, *88*, 801.

(11) Shaw, R.; Walker, F. E. *J. Phys. Chem.* **1977**, *81*, 2572.

(12) (a) Behrens, R., Jr. *Rev. Sci. Instrum.* **1986**, *58*, 451. (b) Behrens, R., Jr. The Application of Simultaneous Thermogravimetric Modulated Beam Mass Spectrometry and Time-of-Flight Velocity Spectra Measurements to the Study of the Pyrolysis of Energetic Materials. In *Chemistry and Physics of Energetic Materials*; Bulusu, S. N., Ed.; Proceedings of the NATO Advanced Study Institute, Vol. 309; Kluwer Academic Publishers: Dordrecht, The Netherlands, 1990; p 327.

(13) Behrens, R., Jr. *Int. J. Chem. Kinet.* **1990**, *22*, 135.

(14) Bulusu, S.; Autera, J. R.; Axenrod, T. *J. Labelled Comp. Radiopharm.* **1980**, *17*, 707.

(15) Boyer, J. H.; Kumar, G. *J. Labelled Compd. Radiopharm.* **1985**, *22*, 1.

(16) Brockman, F. J.; Downing, D. C.; Wright, G. F. *Can. J. Res.* **1949**, *27B*, 469.

(17) Behrens, R., Jr. *Int. J. Chem. Kinet.* **1990**, *22*, 159.

(18) Bulusu, S.; Autera, J. R.; Graybush, R. J. *Proceedings of the 1968 Army Science Conference (OCRD)*; U.S. Army: West Point, NY, 1968; Vol. 2, p 423.

(19) (a) Glidewell, S. M. *Spectrochim. Acta* **1977**, *33A*, 361. (b) Willer, R. L.; Moore, D. W. *Magn. Reson. Chem.* **1988**, *26*, 95.

(20) (a) Nigenda, S. E.; McMillen, D. F.; Golden, D. M. *J. Phys. Chem.* **1989**, *93*, 1124. (b) Fluornoy, J. M. *J. Chem. Phys.* **1962**, *36*, 1106.

(21) Melius, C. F.; Binkley, J. S. *Proceedings of the 21st Symposium (International) on Combustion*; 1987; The Combustion Institute: Pittsburgh, PA, 1988; p 1953.

DISTRIBUTION LIST

Commander
Armament Research, Development and Engineering Center
U.S. Army Armament, Munitions and Chemical Command
ATTN: SMCAR-IMI-I (3)
SMCAR-AEE (3)
SMCAR-AEE-B (5)
Picatinny Arsenal, NJ 07806-5000

Commander
U.S. Army Armament, Munitions and Chemical Command
ATTN: AMSMC-GCL (D)
Picatinny Arsenal, NJ 07806-5000

Administrator
Defense Technical Information Center
ATTN: Accessions Division (12)
Cameron Station
Alexandria, VA 22304-6145

Director
U.S. Army Material Systems Analysis Activity
ATTN: AMXSY-MP
Aberdeen Proving Ground, MD 21005-5066

Commander
Chemical Research, Development and Engineering Center
U.S. Army Armament, Munitions and Chemical Command
ATTN: SMCCR-MSI
Aberdeen Proving Ground, MD 21010-5423

Director
U.S. Army Edgewood Research, Development and Engineering Center
ATTN: SCBRD-RTT (Aerodynamics Technical Team)
Aberdeen Proving Ground, MD 21010-5423

Director
Ballistic Research Laboratory
ATTN: AMXBR-OD-ST
Aberdeen Proving Ground, MD 21005-5066

Chief
Benet Weapons Laboratory, CCAC
Armament Research, Development and Engineering Center
U.S. Army Armament, Munitions and Chemical Command
ATTN: SMCAR-CCB-TL
Watervliet, NY 12189-5000

Commander
U.S. Army Rock Island Arsenal
ATTN: SMCAR-TL, Technical Library
Rock Island, IL 61299-5000

Director
U.S. Army TRADOC Systems Analysis Activity
ATTN: ATAA-SL
White Sands Missile Range, NM 88002